Multivariable Controller Structure in a Variable Cam Timing Engine with Electronic Throttle and Torque Feedback.

Stephen C. Hsieh[1,2], James S. Freudenberg[1], Anna G. Stefanopoulou[3]

Abstract

By adding an electronic throttle and a torque sensor to an engine equipped with variable cam timing, it is potentially possible to vary cam phasing to improve emissions and fuel economy while preserving the torque response of a conventional non-VCT engine. To do so effectively, however, requires the use of multivariable control. A controller consisting of decentralized individual control loops will not yield satisfactory performance because such a controller cannot compensate for system interactions. Yet, a fully multivariable controller may not prove necessary in order to achieve the desired performance. In this paper, we design linear multivariable controllers at a number of operating points and simplify the resulting controllers by eliminating cross-coupling terms that do not affect the closed loop response. Doing so provides insight useful in tuning controller parameters.

1 Introduction

The use of dual-equal variable cam timing (VCT) in spark-ignited engines to reduce feedgas emissions and improve fuel economy has been documented in the literature [2, 5, 6]. Dual-equal variable cam timing affects the period during which the intake and exhaust valves open and close relative to the crankshaft. When the cam timing is retarded, a portion of the combustion products that would normally be expelled in a conventional non-VCT engine with a mechanical throttle linkage (from here on simply referred to as the *conventional engine*) is retained within the cylinder to be burned again during the next engine cycle. In turn, less fresh air is drawn from the manifold; this translates to operation under higher manifold pressure (*MAP*) for a given load. As a result, hydrocarbon (*HC*) and nitrous oxide (*NOx*) emissions from the engine are lowered while fuel economy is improved.

The structure of the VCT model used by this paper is developed in [5]. In previous work ([1, 5]) it was noted that there are significant interactions between the performance outputs—torque (*TQ*), cam phasing (*CAM*), and air-fuel ratio (*AF*). These interactions impose tradeoffs among drivability, feedgas emissions, and catalytic converter efficiency. In particular, the faster the cam actuator moves, the quicker feedgas emissions are lowered. On the other hand, moving the cam too quickly will result in large deviations from stoichiometric air-fuel ratio as well as hesitation in torque response, both of which are undesirable.

It has been observed that these tradeoffs among drivability, fuel economy, and emissions can be made less severe with the use of electronic throttle [1, 7]. A multivariable controller which controls not only cam phasing but also electronic throttle and fuel injection (Figure 1) has the potential to preserve the feedgas emissions improvements of VCT while maintaining the torque performance of a conventional engine [1]. The additional actuators also allow the use of retarded cam phasing over a larger operating regime of the engine to further lower emissions and improve fuel economy.

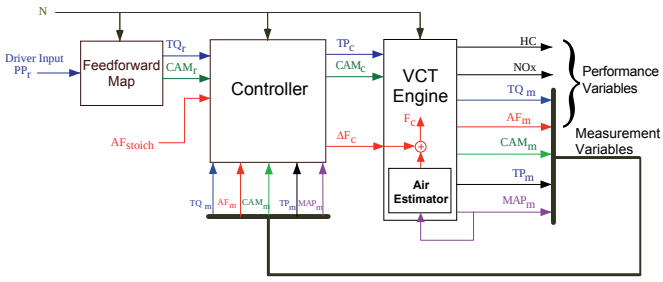

Figure 1: Input/output diagram of the closed-loop VCT engine. *N*=engine speed, *TP*=throttle position, and *F*=fuel.

2 The VCT Engine

2.1 Steady-State Torque Response

While cam retard is beneficial in reducing emissions, it has a detrimental effect on steady state torque as manifold pressure increases. Figure 2 contains the plot of two torque curves as a function of throttle angle. The solid line shows the steady-state torque curve of the conventional engine. In the conventional engine, the cam phasing is fixed at base cam timing ($CAM = 0$) and the throttle position and driver's pedal position are assumed to be equal. The dotted line shows the torque curve of the engine if cam phasing is no longer held constant, but instead scheduled according to a

[1]Electrical Engineering and Computer Science Dept., Univ. of Michigan, Ann Arbor, MI 48109; Support provided by the National Science Foundation (contracts ECS-94-14822 and ECS-98-10242) and Ford Motor Company.

[2]Ford Motor Company, Ford Research Laboratory, PO Box 2053, MD2036 SRL, Dearborn, MI 48121.

[3]Mechanical and Environmental Engineering Dept., Univ. of California, Santa Barbara, CA 93106. Support provided by the National Science Foundation (contract ECS-97-33293) and Ford Motor Company.

particular feedforward cam map. (A detailed description of such a map is found in [1].) For a given throttle position, cam retard may have a dramatic impact on torque, depending on the shape of the cam map. One of the objectives of the closed-loop system is to recover the conventional engine torque curve (solid line) through the use of electronic throttle despite aggressive cam retard. This is done by increasing the electronic throttle angle until the corresponding torque is equivalent to that of the conventional engine. For example, if the driver's pedal position is 12 degrees, the conventional engine would generate 178 Nm of torque, since the pedal and throttle are assumed equal. However, if we retard the cam and follow the trajectory of the dotted line, then a throttle angle of 12 degrees would result in only approximately 140 Nm of torque. In order for the closed-loop VCT system with electronic throttle to generate the same steady-state torque as the conventional engine, the controller needs to increase the electronic throttle angle to 28 degrees.

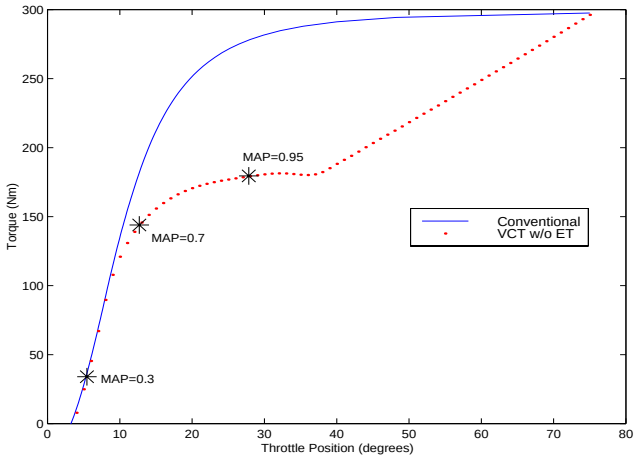

Figure 2: Steady-state torque vs. throttle curves at 1500 RPM of: (1) the conventional engine, and (2) the VCT engine (without electronic throttle) whose cam phasing is scheduled according to a particular cam map.

2.2 Small Signal Analysis

The VCT is a highly interactive multiple-input multiple-output (MIMO) system. This fact implies that a decentralized control system (i.e. cam→cam, throttle→torque, Δfuel→air-fuel ratio) that seems plausible initially may in fact be deficient due to its inability to compensate for these interactions.

To obtain insight into these interactions, we examine open-loop Bode magnitude plots at various operating points. This gives us information about the severity of the interactions in both transient and steady-state conditions. From the Bode plots, we can see that there will be undesirable dynamic interactions from cam phasing to torque and air-fuel ratio, as well as from throttle to air-fuel ratio. Furthermore, the intensity of these undesired interactions varies with operating point. A more detailed analysis of the input/output interactions of the VCT engine is discussed in [1].

Figure 3 shows the open-loop Bode magnitude plots of the VCT engine linearized about three different manifold pressures at 1500 RPM. The inputs to the system are throttle (degrees), cam timing (degrees), and Δfuel (g/intake stroke). The outputs are torque (Nm), cam timing (degrees), and air-fuel ratio (unitless). The A/F measurement was scaled to reflect the importance of small air-fuel ratio deviations from stoichiometry, and the Δfuel input was then scaled so that a unit change in Δfuel resulted in approximately a unit change in scaled air-fuel measurement. The remaining inputs and outputs were left in engineering units.

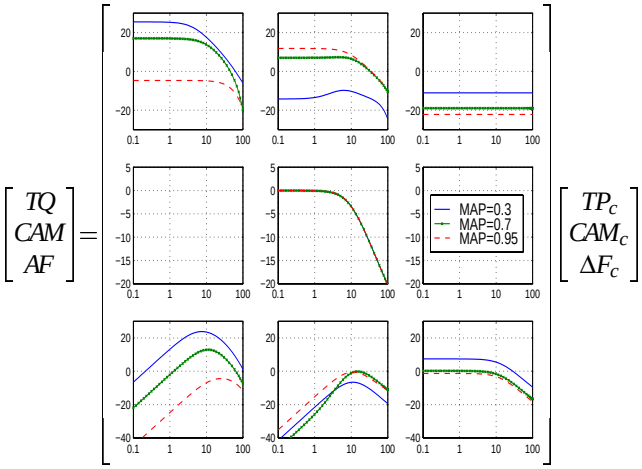

Figure 3: Open-loop Bode magnitude plots for three operating points at 1500 RPM.

There are no steady-state effects of throttle and cam phasing on air-fuel ratio because the open-loop VCT engine contains a feedforward air estimator; in other words, assuming a perfect model of the engine, stoichiometric air-fuel ratio is achieved in *steady-state* if Δfuel=0. The inclusion of an air estimator (whose computed fuel output is still subject to injector and fuel transport delays) in what is considered to be the open-loop plant yields a stable system against which we can benchmark closed-loop system response.

As mentioned earlier, moving the cam actuator will cause transient and possibly steady-state disturbances in torque. This can be seen from the P_{12} plot in Figure 3. Moving either the throttle or cam also causes transient disturbances to air-fuel ratio, as shown in P_{31} and P_{32}, respectively. The P_{21} and P_{23} blocks are empty because changes in throttle and fuel do not affect cam phasing. It should also be noted that the bandwidth of the air-fuel ratio closed loop is limited due to the time it takes for exhaust gases to travel from the cylinder to the downstream UEGO sensor. Thus, high-frequency disturbances from both *TP* and *CAM* to *AF* cannot be effectively attenuated by feeding back the *AF* measurement [4].

Observe how the magnitude of these disturbances change with operating point. In the next section, we will see how changes in the plant input/output coupling affects the underlying controller structure necessary to achieve desired closed-loop performance.

3 Multivariable Controller Structure

In [1], a linear multivariable (MIMO) controller was used to illustrate closed-loop system behavior for a VCT engine with electronic throttle and torque sensor. The desired closed-loop specifications were to use cam retard effectively to reduce emissions and fuel economy, while preserving the dynamic torque response characteristics of the open-loop, conventional engine. (The specific methodology used to synthesize these controllers was LQG, although other MIMO methodologies could also have been used.) Controllers designed by modern synthesis methods may be of high order and thus difficult to implement due to memory and computational constraints. It may also prove difficult to tune these controllers without any additional insight into how they compensate for the interactions in the plant. In this section, we will decompose linear multivariable controllers into separate transfer functions from each controller input to output. By zeroing out certain transfer functions and comparing the performance of these simplified MIMO controllers against their original MIMO counterparts, we will be able to better understand the structure of both the plant and controller. The simplified controller may also be more suited for practical implementation and ease of tuning. Another benefit of this analysis will be to justify the use of multivariable control over decentralized (single-loop) control.

A controller designed using LQG may be viewed as consisting of dynamical blocks from both the error and reference measurements, as well as blocks from additional measurements used by the observer that are not directly regulated. Such a discrete-time full-dimensional state estimator with state feedback (augmented with integrators for integral control) has the form

$$\begin{bmatrix}\hat{x}(k+1)\\ q(k+1)\end{bmatrix} = \begin{bmatrix}\hat{A}-L\hat{C}+(L\hat{D}-B)K_1 & (L\hat{D}-\hat{B})K_2\\ 0 & I\end{bmatrix}\begin{bmatrix}\hat{x}(k)\\ q(k)\end{bmatrix} + \begin{bmatrix}-L_1 & L_1 & L_2\\ -I & 0 & 0\end{bmatrix}\begin{bmatrix}e(k)\\ r(k)\\ m(k)\end{bmatrix} \quad (1)$$

$$u(k) = -K_1\hat{x}(k) - K_2 q(k), \quad (2)$$

where

$\hat{x}, q$	=	observer and integrator states
$\hat{A},\hat{B},\hat{C},\hat{D}$	=	A, B, C, D of the plant
L_1, L_2	=	observer gains
K_1, K_2	=	state feedback gains
e, r	=	error and reference signals
m	=	additional measurements used by observer
u	=	control signal.

If the regulated outputs of the plant are denoted by y, then the error signal, e, is the difference between the reference and measured values (i.e. $e = r - y$).

Represented as a matrix of single input/output transfer functions, the controller takes on the following form in the context of the VCT engine:

$$\begin{bmatrix}TP_c\\ CAM_c\\ \Delta F_c\end{bmatrix} = \left[\begin{array}{ccc|ccc|cc} C_{11}&C_{12}&C_{13}&C_{14}&C_{15}&C_{16}&C_{17}&C_{18}\\ C_{21}&C_{22}&C_{23}&C_{24}&C_{25}&C_{26}&C_{27}&C_{28}\\ C_{31}&C_{32}&C_{33}&C_{34}&C_{35}&C_{36}&C_{37}&C_{38}\end{array}\right] \left[\begin{array}{c} TQ_{err}\\ CAM_{err}\\ AF_{err}\\ \hline TQ_{ref}\\ CAM_{ref}\\ AF_{ref}\\ \hline TP_{meas}\\ MAP_{meas}\end{array}\right] \quad (3)$$

Controller elements corresponding to the error signals are feedback terms. Those corresponding to the reference signals are feedforward terms. The remaining terms are used for state estimation by the observer.

In general, all terms in the multivariable controller will be nonzero. However, many of them may be insignificant. Eliminating controller terms, where appropriate, may reduce controller complexity and will ease the computational burden associated with the controller. In addition, the controller will be easier to understand and to schedule across operating regimes. The criteria for eliminating a term from Equation 3 is that it must not significantly affect the closed-loop performance. It will turn out that in all the cases examined in this paper, the elements corresponding to the error terms are sufficient to preserve the behavior of the full-order MIMO controller (i.e. $C_{ij} = 0$ for $i = 1\ldots3,\ j = 4\ldots8$). Therefore, these terms are dropped to conserve space.

The following subsections examine the controller structure for three different operating points at 1500 RPM: $MAP = 0.3$, 0.7, and 0.95 bar. The location of these points on the VCT torque curve is designated by *'s in Figure 2.

3.1 MAP=0.3 bar

At a linearization point of $MAP = 0.3$ bar ($TP = 5.5$ degrees, $CAM = 10.5$ degrees), at 1500 RPM, our MIMO controller which meets closed-loop system requirements can be reduced to

$$\begin{bmatrix}TP_c\\ CAM_c\\ \Delta F_c\end{bmatrix} = \begin{bmatrix}C_{11}&C_{12}&0\\ 0&C_{22}&0\\ C_{31}&0&C_{33}\end{bmatrix}\begin{bmatrix}TQ_{err}\\ CAM_{err}\\ AF_{err}\end{bmatrix}. \quad (4)$$

Many of the blocks can be removed without any performance degradation because the cross-coupling effects between the actuators are not severe. This can be verified by examining the $MAP = 0.3$ bar lines of the open-loop Bode magnitude plot in Figure 3.

From the Bode plots, it can be seen that at this linearization point, the gain of the P_{11} ($TP \rightarrow TQ$) block is approximately 30–40 dB greater than P_{12} ($CAM \rightarrow TQ$) or P_{13} ($F_c \rightarrow TQ$). Thus, throttle has the strongest actuation authority over torque. As for P_{21} and P_{23}, these plots are empty

because the cam actuator is neither affected by TP nor ΔF in open loop. Also note that CAM has little effect on TQ and no effect on AF in steady-state[1]. From P_{31} and P_{32}, it is evident that AF is affected by transient changes in both TP and CAM. However, there are no steady-state effects of throttle and cam phasing on air-fuel ratio due to the built-in air estimator mentioned previously.

By understanding the structure of the plant, we can explain why only C_{11}, C_{12}, C_{22}, C_{31} and C_{33} are necessary. The diagonal feedback terms are needed because they track the TQ, CAM, and AF reference signals. Because the throttle and cam actuators have approximately the same bandwidth, and it takes time for throttle to affect torque, moving throttle based on feedback alone is not sufficient to reject cam disturbances on torque. Thus, the C_{12} ($CAM_{err} \rightarrow TP_c$) term is effectively a "feedforward" term in the controller which moves the throttle to compensate for the effect of cam phasing on air flow. The same is true for C_{31} ($TQ_{err} \rightarrow F_c$); there is significant delay in measuring air-fuel ratio—in order to better regulate A/F, it is necessary to use a feedforward element to the Δfuel command to compensate for the disturbance caused by throttle movement.

Figure 4 shows the simplified structure that preserves the behavior of the full MIMO controller.

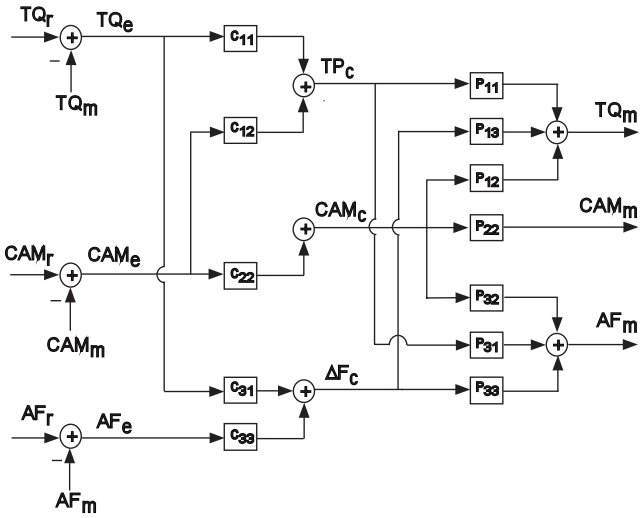

Figure 4: Simplified controller and plant block diagram for the $MAP = 0.3$ operating point.

C_{13} and C_{23} can be eliminated because the air-fuel ratio measurement is significantly delayed; information from AF_{err} comes too late to be of any use to throttle or cam. C_{21} is not used because at this linearization point, manifold pressure is low (sonic flow regime). Therefore, the intake air flow is determined only by throttle angle, and the effect of cam phasing on air flow (thereby affecting torque and air-fuel ratio) is minimal. Thus, with C_{12} already rejecting the disturbance of cam on air flow, air-fuel ratio is already decoupled from the cam actuator and C_{32} can be eliminated.

3.2 MAP=0.7 bar

At the operating point of $MAP = 0.7$ bar ($TP = 12.7$ degrees, $CAM = 37.7$ degrees), the behavior of the engine is noticeably different than at $MAP = 0.3$ bar. This operating point corresponds to operation under subsonic flow. The open-loop Bode magnitude plots for $MAP = 0.7$ in Figure 3 show that the relative authorities of the actuators on the output variables have changed.

Cam phasing now has a much stronger impact on torque, and a slightly higher peak in air-fuel ratio. The peak of the P_{12} ($CAM \rightarrow TQ$) block has increased by 20 dB as compared to the $MAP = 0.3$ case. Similarly, the peak for P_{32} ($CAM \rightarrow AF$), has increased by almost 10 dB. A key difference from the first linearization point is that cam now has greater actuation authority over torque. The DC gain of P_{12} is much larger now due to the fact that at $MAP = 0.7$, manifold pressure is higher than before and intake air flow is now a function of both throttle angle and manifold pressure (cam retard increases manifold pressure).

Another important observation is that the P_{11} ($TP \rightarrow TQ$) and P_{31} ($TP \rightarrow AF$) terms are smaller in magnitude. This means that the authority of throttle on torque and air-fuel ratio has decreased; as manifold pressure increases, the pressure difference across the throttle plate drops, and thus changes in throttle angle have less of an impact on air flow. Clearly, the actuators are now tightly coupled, and disturbances on one loop caused by another will be more difficult to reject.

Naturally, the stronger interactions between actuators at this operating point results in a simplified MIMO controller which contains a different, more populated structure than the $MAP = 0.3$ simplified controller:

$$\begin{bmatrix} TP_c \\ CAM_c \\ \Delta F_c \end{bmatrix} = \begin{bmatrix} C_{11} & C_{12} & 0 \\ C_{21} & C_{22} & 0 \\ C_{31} & C_{32} & C_{33} \end{bmatrix} \begin{bmatrix} TQ_{err} \\ CAM_{err} \\ AF_{err} \end{bmatrix}. \qquad (5)$$

In addition to the controller terms needed for the first operating point, two more terms are now necessary to preserve the closed-loop response of the full MIMO controller. Necessity of the C_{21} and C_{32} terms is due to the increased coupling of cam on torque and air-fuel ratio. The presence of C_{21} means that the controller recognizes the increased authority of cam on torque. In one sense, cam movement causes a larger disturbance on torque. On the other hand, we can now also think of using cam as an additional actuator to improve transient torque regulation. By utilizing C_{21}, the controller can utilize both throttle and cam actuators to affect torque.

With the increased use of cam to assist in torque regulation, the presence of the feedforward term, C_{32}, assists in decou-

[1] In [1], cam phasing was described to have no steady-state effect on torque in sonic flow because cam phasing was assumed to affect only mass air flow into the cylinders. The VCT model used in the present paper has been modified to account for the effect of cam on volumetric efficiency.

pling cam movement from air-fuel ratio by using Δfuel to offset disturbances on air-flow caused by cam movement. This block, along with C_{31}, are important because only Δfuel can be used to regulate air-fuel ratio; the blocks from air-fuel error to throttle command and cam command, C_{13} and C_{23} respectively, continue to be useless because of the time lag involved in measuring air-fuel ratio.

Figure 5 shows the simplified structure that preserves the behavior of the full MIMO controller.

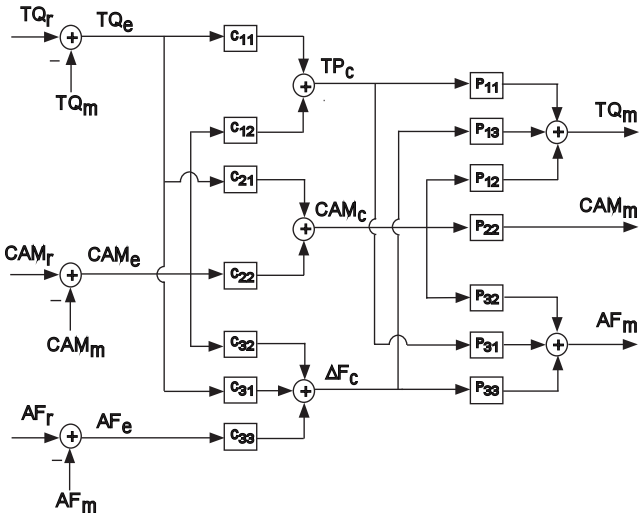

Figure 5: Simplified controller and plant block diagram for the $MAP = 0.7$ operating point.

3.3 MAP=0.95 bar

Operating the VCT engine at $MAP = 0.95$ bar ($TP = 27.8$ degrees, $CAM = 38.1$ degrees), is interesting because we are essentially running the engine under wide-open throttle conditions. We can model mass air flow through the throttle body ($\dot{m}_\theta$), assuming constant flow through a valve opening [3], by

$$\dot{m}_\theta = g_1(MAP, P_o) \cdot g_2(TP) \tag{6}$$

$$g_1(MAP, P_o) = \begin{cases} \left(\frac{2}{\gamma+1}\right)^{\frac{\gamma+1}{2(\gamma-1)}} & \text{if } \frac{MAP}{P_o} \leq 0.528 \\ \left(\frac{2}{\gamma-1}\right)^{\frac{1}{2}} \sqrt{\left(\frac{MAP}{P_o}\right)^{\frac{2}{\gamma}} - \left(\frac{MAP}{P_o}\right)^{\frac{\gamma+1}{\gamma}}} & \\ & \text{if } \frac{MAP}{P_o} > 0.528 \end{cases} \tag{7}$$

$$g_2(TP) = F(1, TP, TP^2, e^{-15TP}), \tag{8}$$

where $\gamma = \frac{c_p}{c_v} = 1.4$ is the ratio of specific heats, TP is throttle angle, MAP is manifold pressure, and P_o is ambient pressure. $F(\cdot)$ in Equation 8 represents a polynomial in TP whose arguments are the basis function.

The throttle affects the engine breathing dynamics only through $g_2(TP)$ of Equation 6. High manifold pressure implies that $\frac{MAP}{P_o} \approx 1$. Thus, from Equations 6 and 7, $\dot{m}_\theta \approx 0$ under high manifold pressure conditions. In other words, when the engine operates in this regime, the throttle has very little control authority. The open-loop Bode magnitude plots for $MAP = 0.95$ in Figure 3 confirm this result visually; despite the fact that we have three physical actuators, one is weak and in fact only two of the three actuators—cam and fuel—are effective.

If throttle has virtually no actuator authority, then the system is close to no longer being controllable in the sense that we cannot control 3 outputs (torque, cam, and air-fuel ratio) independently with only 2 strong actuators (cam and Δfuel). In designing the MIMO controller for this operating point, our primary objective is to preserve the torque response of the conventional engine. Thus, emphasis is placed on reducing torque tracking error as opposed to cam tracking error. With this in mind, the simplified controller which preserves the closed-loop properties of the full MIMO controller turns out to have the form:

$$\begin{bmatrix} TP_c \\ CAM_c \\ \Delta F_c \end{bmatrix} = \begin{bmatrix} 0 & 0 & 0 \\ C_{21} & 0 & 0 \\ C_{31} & 0 & C_{33} \end{bmatrix} \begin{bmatrix} TQ_{err} \\ CAM_{err} \\ AF_{err} \end{bmatrix}. \tag{9}$$

From the lack of any C_{1j} terms, we conclude from the resulting structure that as long as throttle is held near a wide-open position, throttle will not affect any of the outputs and has no authority in this region. Furthermore, the lack of any C_{i2} terms, especially C_{22}, means that the controller no longer tracks desired cam. Instead, the presence of C_{21} means that the controller now uses cam to regulate torque, and C_{31} is a feedforward term to offset disturbances on the air-fuel loop by cam.

Figure 6 shows the simplified structure that preserves the behavior of the full MIMO controller.

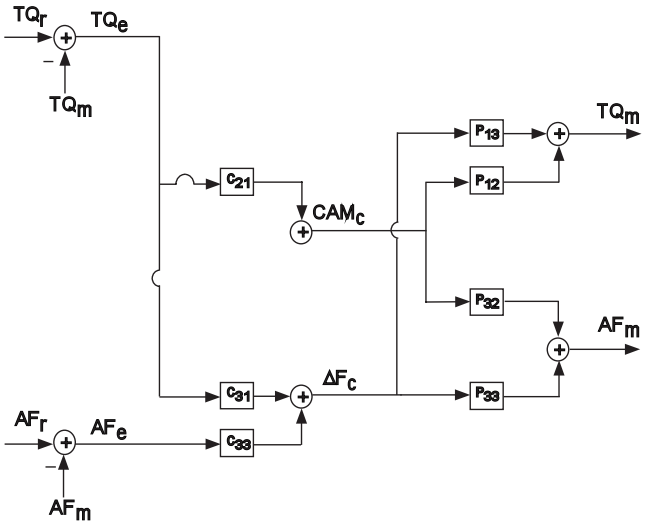

Figure 6: Simplified controller and plant block diagram for the $MAP = 0.95$ operating point.

4 Nonlinear Simulation

A typical nonlinear simulation of the VCT engine at 1500 RPM is shown in Figure 7. This plot contains the time responses of the conventional engine as well as the simplified $MAP = 0.7$ MIMO and decentralized closed-loop systems. Since the full and simplified MIMO controllers behave identically, only the simplified controller is shown.

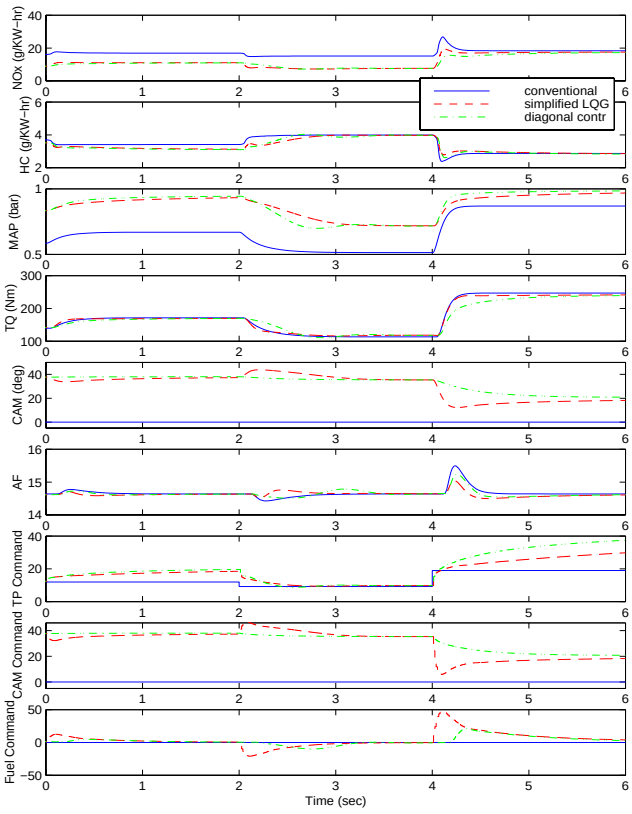

Figure 7: Nonlinear simulation of the response to a series of pedal steps ($PP = 12 \rightarrow 9 \rightarrow 19$ degrees) at 1500 RPM for: (1) the conventional engine, (2) simplified $MAP = 0.7$ MIMO controller, and (3) $MAP = 0.7$ controller with diagonal (C_{11}, C_{22}, C_{33}) terms only.

Through the use of VCT and electronic throttle compensation, the closed-loop MIMO system is able to match the conventional engine torque response while operating at higher manifold pressure to improve fuel economy, lowering emissions, and minimizing deviations from stoichiometric air-fuel ratio. If a diagonal (decentralized) controller is used instead (i.e. torque tracking using throttle, cam tracking using cam, and air-fuel ratio tracking using Δfuel), torque performance suffers. This is because in a decentralized design, the cam actuator cannot be used to regulate torque. Since the throttle actuator loses authority as cam is retarded and manifold pressure increases, it becomes increasingly difficult to track a torque reference by using only throttle. Unlike the MIMO controller, which can advance cam to increase torque, the diagonal controller can only increase the throttle with little effect.

Work is currently underway to verify these simulation results experimentally on a dynamometer-mounted VCT engine with electronic throttle and inline torque sensor.

5 Conclusion

We have shown that the VCT engine is a highly interactive multivariable system. However, it is possible to preserve the torque response of a conventional engine while improving emissions and fuel economy through the joint use of electronic throttle and cam phasing in conjunction with torque feedback.

To better understand what cross-coupling terms are needed in the controller to decouple the inputs of the plant, we can use multivariable controller design methodology to design controllers that achieve the desired closed-loop response and then analyze the resulting structure. We have shown in this paper that it can provide us with valuable insights about the structural requirements of the controller. This information can then be applied to other control design techniques, making the design process for multivariable systems easier and reducing the number of parameters that need to be tuned.

References

[1] S. C. Hsieh, A. G. Stefanopoulou, J. S. Freudenberg, and K. R. Butts, "Emission and Drivability Tradeoffs in a Variable Cam Timing SI Engine with Electronic Throttle," Proc. 1997 Amer. Contr. Conf., pp. 284-288, Albuquerque, 1997.

[2] G. B. Kirby Meacham, "Variable Cam Timing as an Emission Control Tool," SAE Paper No. 700645.

[3] J. M. Novak, "Simulation of the Breathing Processes and Air-Fuel Distribution Characteristics of Three-Valve, Stratified Charge Engines," SAE Paper No. 770881.

[4] A. G. Stefanopoulou, K. R. Butts, J. A. Cook, J. S. Freudenberg and J. W. Grizzle, "Consequences of Modular Controller Development for Automotive Powertrains: A Case Study," Proc. 1995 Conf. on Decision and Control, pp. 768-773, New Orleans, 1995.

[5] A. G. Stefanopoulou, J. A. Cook, J. S. Freudenberg, J. W. Grizzle, "Control-Oriented Model of a Dual Equal Variable Cam Timing Spark Ignition Engine," ASME Journal of Dynamic Systems, Measurement, and Control, vol. 120, pp. 257-266, 1998.

[6] R. A. Stein, K. M. Galietti, and T. G. Leone, "Dual Equal VCT—A Variable Camshaft Timing Strategy for Improved Fuel Economy and Emissions," SAE Paper No. 950975.

[7] H.-M. Streib and H. Bischof, "Electronic Throttle Control: A Cost Effective System for Improved Emissions, Fuel Economy, and Drivability", SAE Paper No. 960338.